





Cite this: *Chem. Commun.*, 2022, 58, 3957

Received 17th January 2022,
Accepted 22nd February 2022

DOI: 10.1039/d2cc00318j

rsc.li/chemcomm

Multifunctional fluorescent probe for effective visualization, inhibition, and detoxification of β -amyloid aggregation *via* covalent binding†

Ziqi Zhang, Yue Cao, Qiong Yuan, Chenghui Liu,  Xinrui Duan * and Yanli Tang *

A multifunctional reactive fluorescent probe DTB was constructed for biosensing, aggregation inhibition, and toxicity alleviation of β -amyloid. The synergistic effect of hydrophobic interaction and covalent interaction makes DTB have more stable binding and better selectivity to $A\beta$. The detoxification effect of DTB on $A\beta$ aggregates was also verified in live nerve cells and microglia cells. Furthermore, DTB exhibits an excellent staining of $A\beta$ plaques.

Alzheimer's disease (AD), as a typical neurodegenerative disease, is afflicting an increasing population. The possibility of AD increases with aging, and it poses a serious threat to human health. The plaques formed by misfolding and deposition of β -amyloid ($A\beta$) in the brain are directly linked with the destruction of memory and motor neuron function.¹ $A\beta$ s are composed of 39–43 amino acids and have various aggregate forms depending on the degree of aggregation.² As a therapeutic target of AD, the current research on $A\beta$ mainly focuses on the detection and imaging of $A\beta$,³ as well as inhibition and degradation of aggregates to alleviate the toxicity of $A\beta$.⁴

A variety of probes have been designed and synthesized for sensing $A\beta$, such as peptides,⁵ small molecules,⁶ nano-materials,⁷ polymers,⁸ *etc.* Organic small-molecule fluorescent probes are quite advantageous in detecting $A\beta$ aggregation and elucidating its biological functions due to its defined structure and certain structure–activity relationship.⁶ Various fluorescent probes and their derivatives have been continuously developed.⁹ Although these fluorescent probes possessed recognition ability for $A\beta$ aggregation, these probes performed mainly by noncovalent interactions (π – π stacking, H-bonding, electrostatic interactions and hydrophobic interactions), which are

unstable and sensitive to interference. Therefore, the design of a probe with the ability of effective visualization and inhibition of $A\beta$ aggregation by covalent bonding still is highly challenging.¹⁰

Bithiophene has a conjugated structure with relative flexibility. The addition of electron-donating and electron-withdrawing groups on both sides could produce a fluorophore that responds to rigid environments.¹¹ When such probes bind to amyloid protein through electrostatic and hydrophobic interactions, the rigidity of the molecular structure is enhanced. Therefore, the energy attenuation resulting from non-radiative transition is reduced and the quantum yield is greatly increased. Covalent bonding will lock the probe with the target, resulting in further restriction of the free rotation of the probe.⁸

The spontaneous amino-yne click reaction has been widely used in hydrogel preparation,¹² surface immobilization,¹³ macromolecule synthesis¹⁴ and stimuli-responsive drug delivery¹⁵ since it was first reported in 2017.¹⁶ It was speculated that the reaction prefers organic solvents over aqueous solution. Therefore, we believed that the addition of the ethynyl group on the bithiophene would allow the probe to specifically and covalently bond to $A\beta$ aggregates, which provides a necessary hydrophobic environment for the reaction. The covalent binding of the probe may interfere with the delicate folding and formation of $A\beta$ aggregation, producing effective inhibition of $A\beta$ aggregation.

Herein, we developed a fluorescent “turn on” probe (DTB) that can visualize and inhibit the aggregation of $A\beta$ (Fig. 1). The DTB was designed by installing an *N,N*-diethylphenylamine group as an electron-donating group and a carbonyl activated ethynyl group as a covalent binding group into each of the 5' positions of the 2,2'-bithiophene molecules, respectively. Due to the free rotation of all intramolecular single bonds, the energy of the excited state of DTB dissipated in a non-radiative form, leading to extremely low fluorescence. The diethylaminophenyl bithiophene would selectively bind to the hydrophobic part of the $A\beta$ aggregates, and the carbonyl-activated ethynyl group can react with the nearby amino group in the $A\beta$ aggregates through a catalyst-free amino-yne click reaction to form a stable covalent bond.¹³

Key Laboratory of Analytical Chemistry for Life Science of Shaanxi Province,
Key Laboratory of Applied Surface and Colloid Chemistry,
Ministry of Education, School of Chemistry and Chemical Engineering,
Shaanxi Normal University, Xi'an 710119, P. R. China.

E-mail: duanxr@snnu.edu.cn, yiltang@snnu.edu.cn; Fax: +86-29-81530727

† Electronic supplementary information (ESI) available: Experimental section, synthesis of DTB precursor and DTB, ¹H NMR, ¹³C NMR and HR-MS data, and Fig. S1–S20. See DOI: 10.1039/d2cc00318j

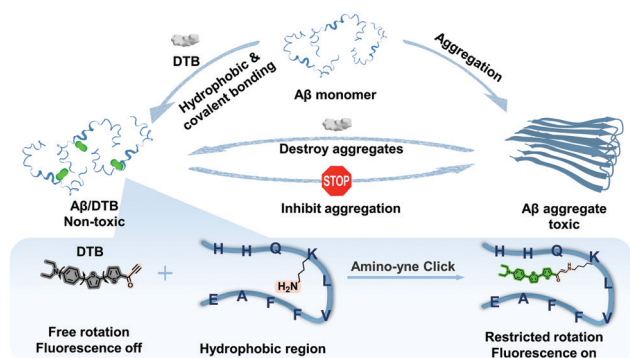


Fig. 1 Schematic illustration of the interaction of DTB and A β .

Both the hydrophobic binding and formation of the covalent bond would reduce the free rotation of the probe and lead to an enormous increase of the fluorescence intensity. Furthermore, DTB can inhibit the formation of A β aggregates and showed a significant detoxification ability. Therefore, we constructed a multifunctional fluorescent “turn on” small molecule probe, which provides a new approach for biosensing, imaging, diagnosis, and therapy of AD.

The synthetic route and characterization of DTB were shown in Fig. S1–S4 (ESI[†]). The absorption peak of DTB is at 440 nm and no obvious emission was detected in PBS solution (Fig. 2a), which indicates that DTB has an extremely low fluorescence background. The optimized excited state geometry (theoretical calculation by TDDFT, Fig. S5, ESI[†]) was almost a planar structure (three aromatic rings are in the same plane), thus the free rotating of the single bonds would break the planar structure and result in extremely low fluorescence. The ethynyl group in DTB can react with the amino group spontaneously in THF but not in PBS solution (Fig. S6–S8, ESI[†]). This property lay the foundation for the selective reaction between DTB and A β or its aggregates but not any amines in the biological environment. Namely, spontaneous amino-yne click reaction may

occur effectively only in the hydrophobic region of A β or A β aggregates.

Then, the fluorescence response of DTB for A β was investigated. In the absence of A β , the probe (1.0 μ M) showed an extremely low background fluorescence. As we expected, the fluorescence intensity of DTB significantly enhanced with the increase of A β concentration (Fig. 2b). The fluorescence response maintained a good linear relationship in the range of 0–28 μ M A β and reached a plateau when A β reached 35 μ M (Fig. 2c). Due to the hydrophobic binding and covalent reaction restricting the free rotation of the single bond in DTB, the fluorescence intensity of DTB increased greatly. The fold change of fluorescence is surprisingly \sim 1084 times. A limit of detection as low as 19 nM was achieved ($LOD = 3S/\sigma$), which is lower than that of previously reported fluorescent probes, such as 50 nM¹⁷ and 51.9 nM.¹⁸ In addition, the absolute quantum yield increased from 2.8% to 37.2% after incubation with A β . The fluorescence changes can be easily observed under a UV lamp (inset photo in Fig. 2b). Meanwhile, the fluorescence of DTB with A β increased rapidly within 30 min, confirming a quick response of the probe (Fig. S9, ESI[†]). The selectivity of the probe towards A β was studied by using common proteins and typical amino acids. Proteins with different isoelectric points (pI) or molecular weights were selected to rule out the effect of electrostatic interaction or molecular weight. As shown in Fig. 2d, the fluorescence response of DTB was neglectable except for A β , which confirmed the high specificity of DTB for A β sensing.

Next, the interaction between DTB and A β aggregates was investigated. The classic A β aggregates indicator Thioflavin T (ThT) was used to indicate the formation of aggregates. The A β was preincubated for 12 h to form A β aggregates and confirmed by the increase of the fluorescence of ThT at 486 nm (Fig. S10, ESI[†]). Interestingly, when DTB was added, the fluorescence of ThT decreased significantly. In the meantime, the fluorescence of DTB at 550 nm appeared and the intensity of DTB gradually increased while the ThT intensity gradually decreased (Fig. 2e and Fig. S11, ESI[†]). This result suggested a much stronger binding between DTB and A β than ThT, which made DTB a potential disruptor for A β aggregation. As shown in Fig. 2f, the fluorescence intensity of DTB increased proportionally with the concentration of A β aggregates in the range of 0–50 μ M. And the fold change of fluorescence reached \sim 728 times at 50 μ M. These results suggested that DTB can also bind to A β aggregates through hydrophobic and covalent bonds, significantly enhancing the fluorescence of DTB.

Furthermore, to verify the covalent interaction between DTB and A β , molecular docking of DTB with A β monomers and A β aggregates was performed. The results indicated that Lys-16 or Lys-28 was the possible reacting lysine residue of DTB (Fig. S12, ESI[†]). Therefore, the KLVFFAE (A β 16–22) fragment was selected as a simplified model of A β for ¹H NMR analysis, which was the hydrophobic core of A β . As shown in Fig. 3a, after the reaction of KLVFFAE with DTB at room temperature, new peaks appeared at δ 3.07 ppm when compared with the methylene protons on lysine (K16) (δ = 2.69 ppm). Moreover, these peaks remained unchanged when the temperature increased, which

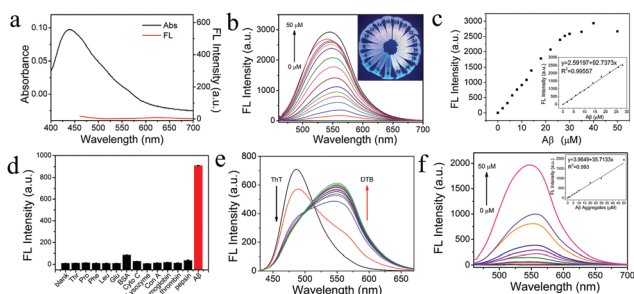


Fig. 2 (a) UV-Vis absorption and fluorescence spectra of DTB. (b) Fluorescence spectra of DTB incubated with different concentrations of A β . The inset is the photographs under a portable UV lamp of these samples. (c) Intensity changes of DTB after incubation with A β . The inset shows the linear correlation between intensity and concentration of A β . (d) Selectivity of DTB towards A β . (e) Fluorescence spectra over time after addition of DTB to A β /ThT solution that was preincubated for 12 h. (f) Fluorescence spectra of DTB after incubating with different concentrations of preformed A β aggregates. The inset is the linear relationship between the fluorescence intensity and A β aggregate concentration.

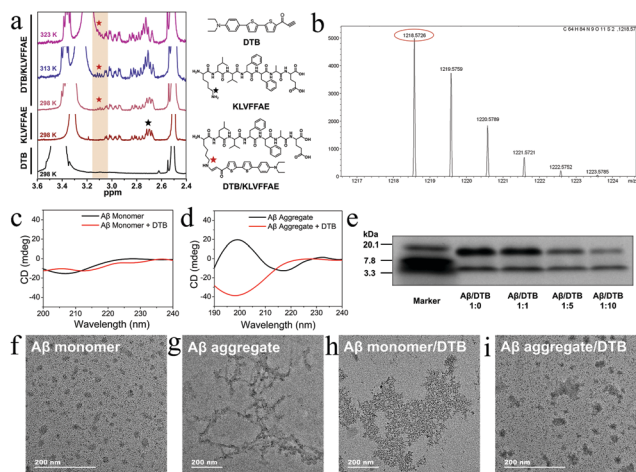


Fig. 3 (a) ^1H NMR spectra of DTB, KLVFFAE, and the DTB/KLVFFAE complex at 298, 313, 323 K. (b) HR-MS spectrum of DTB/KLVFFAE. The CD spectra of the A β monomer (c) and A β aggregates (d) with or without DTB. (e) SDS-PAGE gel electrophoresis of A β incubated with DTB at different molar ratios. (f–i) TEM images of A β monomer (f), A β aggregate (g), A β monomer/DTB (h) and A β aggregate/DTB (i) incubated for 12 h.

indicated that the amino group on lysine reacted with the ethynyl group on DTB to form a strong covalent bond.⁸ Additionally, HR-MS was obtained for confirmation (Fig. 3b). The molecular ion peak at 1218.5726 (m/z) belonging to the covalent reaction product (calcd 1218.5733) of DTB and KLVFFAE peptide was detected.

The formation of a β -sheet structure is a characteristic of A β aggregation to form fibers, and this secondary conformation change can be detected by CD spectrometry. As shown in Fig. 3c, the A β monomer presents a random coil state with or without DTB. After forming the A β aggregate, a positive peak around 198 nm and a negative band around 217 nm appeared, indicating a typical β -sheet structure (Fig. 3d).⁸ The CD spectrum of the A β aggregate with DTB only shows a negative band at 198 nm, which indicates that DTB can destroy the β -sheet structure of the A β aggregates, namely inhibiting its aggregation. To further confirm the inhibition effect of DTB on A β aggregation, SDS-PAGE was performed. As shown in Fig. 3e and Fig. S13 (ESI †), the bands of A β aggregates appeared from 7.8 to 20.1 kDa. When A β was incubated with DTB at different molar ratios of 1:1, 1:5, and 1:10, the bands of A β aggregates from 7.8 to 20.1 became weaker gradually. This result confirmed that the conversion of A β monomers to aggregates was inhibited by DTB.

For further evaluation, TEM imaging of the A β aggregates with or without DTB was conducted to directly observe the morphological changes. After 12 h of preincubation, A β exhibited a typical morphology of aggregation and formed A β fibrils (Fig. 3g). No fibrils were observed from the A β monomer (Fig. 3f) or A β monomer/DTB (5:1, Fig. 3h). As we expected, there were also no fibrils in the A β aggregate/DTB group (5:1, Fig. 3i). Moreover, even when the incubation time extended to 120 h, DTB still showed an excellent inhibitory effect on the formation of A β aggregates (Fig. S14, ESI †). These results indicated that DTB can not only inhibit the formation of fibrous A β aggregates but also

disassemble and disperse the formed A β aggregates, effectively curbing the possibility of A β further aggregation.

As a common model for *in vitro* study of neurological diseases, PC-12 cells were used to study the detoxification effect of the probe on A β aggregates.¹⁹ The cytotoxicity of DTB for PC-12 cells was confirmed as neglectable (Fig. S15, ESI †). The incubation with 30 μM A β results in only 20% left in PC-12 cells (Fig. 4b), implying high cytotoxicity of A β .^{7,8} In the presence of both A β and DTB, the cell viability was kept at 90% after 48 h, which indicates a significant detoxification effect of DTB for A β . PI staining also supports the detoxification effect (Fig. S16, ESI †). Red fluorescence of PI was only observed in cells treated with A β . With DTB and A β , only a few cells were stained by PI. This difference can be easily observed in Fig. 4c. These results showed that DTB had a significant detoxification effect on the cytotoxicity of A β .

The capability of DTB to prevent PC-12 cells from toxic attack by A β aggregates was further evaluated by ThT imaging. As shown in Fig. S17 (ESI †), clear green fluorescence was measured from the group incubated with A β and ThT, which showed significant A β adhesion on PC-12 cells after 12 h of incubation. In contrast, very weak orange fluorescence was observed, indicating very little A β adhesion after the treatment of the cells with A β /DTB for 6 h. Even at 12 h, the A β adhesions remained negligible. When DTB is covalently bound to A β , the formation of A β /DTB locks those free A β , creating steric hindrance and preventing A β aggregation, thereby reducing A β adhesion on PC-12 cells.

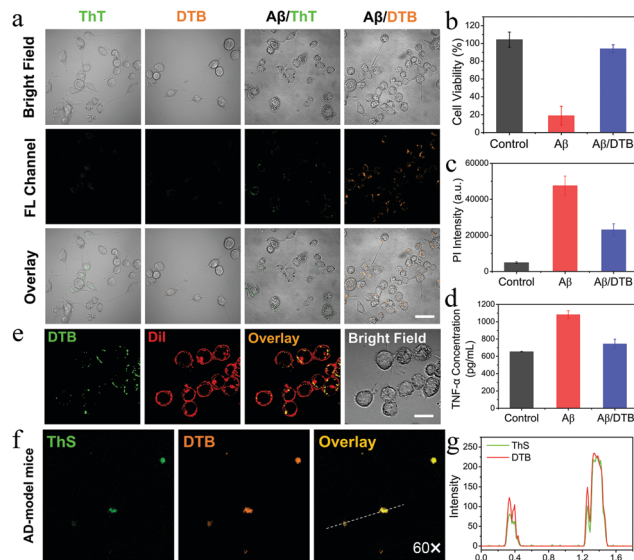


Fig. 4 (a) The CLSM images of BV-2 after being incubated with A β /ThT or A β /DTB for 24 h. The scale bar is 40 μm . (b) Cell viability of PC-12 cells after treatment with A β or A β /DTB. (c) Quantification of PI fluorescence intensity (in Fig. S15, ESI †) of PC-12 cells treated with A β . (d) Quantitative analysis of the TNF- α level of BV-2 cells after different stimuli by ELISA. (e) Colocalization imaging of BV-2 cells treated with A β /DTB and Dil. The scale bar is 20 μm . (f) Histological staining of the brain slices in the hippocampus region from AD-model (APP/PS1 transgenic) mice using ThS and DTB. (g) The intensity profiles of the linear regions of interest (white line) cross the brain slices.

Although the DTB reduced the cytotoxicity of A β on PC-12 cells, the A β /DTB complex is a new “misfolding” product. Its timely and effective removal is also worth investigating.²⁰ The elimination of A β involved microglia.²¹ The mouse microglial BV-2 cells were selected as the model cell line in the phagocytosis study. It is worth noticing that the cytotoxicity of A β aggregates will cause the microglia to secrete TNF- α , and ultimately make the microglia lose the ability to phagocytose A β .²² The cytotoxicity of DTB to BV-2 was negligible according to the MTT assay (Fig. S18, ESI[†]). In addition, the cytotoxicity of A β and A β /DTB towards microglia cells was also investigated. As shown in Fig. S19 (ESI[†]), A β aggregates did not cause obvious toxicity to BV-2 cells, which was different from PC-12 cells. Moreover, the formation of an A β /DTB complex also enhanced the cell viability of BV-2 cells. The phagocytosis of the A β /DTB complex by BV-2 cells was significantly higher than A β (stained with ThT) after incubation for 24 h (Fig. 4a). Quantification of TNF- α levels by ELISA was consistent with fluorescence imaging (Fig. 4d). The secretion of TNF- α was high when BV-2 cells were exposed to A β , while sharply reduced in the presence of DTB. Colocalization imaging of A β /DTB and Dil (a cell membrane dye) shows that the A β /DTB is mainly located on the cell membrane (Fig. 4e). This was consistent with previous reports that A β preferentially started to aggregate at the region where membrane protrusions frequently occur.²³ These results indicate that the DTB prevents microglia cells from losing the ability of phagocytosis by avoiding the upregulation of TNF- α .

To evaluate the applicability of DTB for A β recognition, brain slices from AD-model (APP/PS1 transgenic) mice and wild-type mice were used to perform *in vitro* fluorescent staining of A β . Thioflavin-S (ThS) as a gold standard probe was used for A β marking. As expected, A β in the brain slices of the AD-model mice was successfully observed by DTB (Fig. 4f), while almost no fluorescence was observed in the wild-type mice brain slices (Fig. S20, ESI[†]). The co-staining of DTB with ThS confirmed the great selectivity of DTB to A β (Fig. 4g).

In conclusion, the fluorescent probe DTB was successfully developed for the effective visualization and inhibition of β -amyloid aggregation *via* the amino-yne click reaction. DTB presented extremely low background fluorescence due to the free rotation of all intramolecular single bonds. An enormous fluorescence increase was observed after DTB binding with A β aggregates. DTB not only bound to A β monomers to prevent the formation of aggregates but also destroyed A β aggregates, alleviated the neurotoxicity of A β aggregates, and efficiently restored the A β -clearing ability of microglia. Furthermore, this probe exhibited an excellent staining of A β plaques. Therefore, this work provides insight into the design of fluorescent probes for A β -targeted biosensing, imaging, and therapy.

We thank the financial support from the National Natural Science Foundation of China (Grants 21974084, 22174091), Innovation Capability Support Program of Shaanxi (Program no. 2021TD-42), and Fundamental Research Funds for the Central Universities (No. GK202002013, GK202101001).

Conflicts of interest

The authors declare no competing financial interest.

Notes and references

- M. Goedert, *Science*, 2015, **349**, 1255555.
- W. Qiang, W. M. Yau, J. X. Lu, J. Collinge and R. Tycko, *Nature*, 2017, **541**, 217–221.
- J. Y. Shao, S. H. Wu, J. Ma, Z. L. Gong, T. G. Sun, Y. Jin, R. Yang, B. Sun and Y. W. Zhong, *Chem. Commun.*, 2020, **56**, 2087–2090.
- A. Iscen, C. R. Brue, K. F. Roberts, J. Kim, G. C. Schatz and T. J. Meade, *J. Am. Chem. Soc.*, 2019, **141**, 16685–16695.
- N. Pradhan, D. Jana, B. K. Ghorai and N. R. Jana, *ACS Appl. Mater. Interfaces*, 2015, **7**, 25813–25820.
- A. Aliyan, N. P. Cook and A. A. Marti, *Chem. Rev.*, 2019, **119**, 11819–11856.
- Y. Zhao, J. Cai, Z. Liu, Y. Li, C. Zheng, Y. Zheng, Q. Chen, H. Chen, F. Ma, Y. An, L. Xiao, C. Jiang, L. Shi, C. Kang and Y. Liu, *Nano Lett.*, 2019, **19**, 674–683.
- H. Sun, J. Liu, S. Li, L. Zhou, J. Wang, L. Liu, F. Lv, Q. Gu, B. Hu, Y. Ma and S. Wang, *Angew. Chem., Int. Ed.*, 2019, **58**, 5988–5993.
- (a) S. D. Quinn, P. A. Dalgarno, R. T. Cameron, G. J. Hedley, C. Hacker, J. M. Lucocq, G. S. Baillie, I. D. Samuel and J. C. Penedo, *Mol. Biosyst.*, 2014, **10**, 34–44; (b) P. Dao, F. Ye, Y. Liu, Z. Y. Du, K. Zhang, C. Z. Dong, B. Meunier and H. Chen, *ACS Chem. Neurosci.*, 2017, **8**, 798–806; (c) K. Pagano, S. Tomaselli, H. Molinari and L. Ragona, *Front. Neurosci.*, 2020, **14**, 619667.
- H. Sun, F. Lv, L. Liu and S. Wang, *ACS Appl. Mater. Interfaces*, 2019, **11**, 22973–22978.
- S. Maity, C. M. Sadowski, J. M. George Lin, C. H. Chen, L. H. Peng, E. S. Lee, G. K. Vegesna, C. Lee, S. H. Kim, D. Mochly-Rosen, S. Kumar and N. Murthy, *Chem. Sci.*, 2017, **8**, 7143–7151.
- O. S. Fenton, J. L. Andresen, M. Paolini and R. Langer, *Angew. Chem., Int. Ed.*, 2018, **57**, 16026–16029.
- Y. Zhang, J. Shen, R. Hu, X. Shi, X. Hu, B. He, A. Qin and B. Z. Tang, *Chem. Sci.*, 2020, **11**, 3931–3935.
- B. He, J. Zhang, J. Wang, Y. Wu, A. Qin and B. Z. Tang, *Macromolecules*, 2020, **53**, 5248–5254.
- P. Wu, X. Wang, Z. Wang, W. Ma, J. Guo, J. Chen, Z. Yu, J. Li and D. Zhou, *ACS Appl. Mater. Interfaces*, 2019, **11**, 18691–18700.
- B. He, H. Su, T. Bai, Y. Wu, S. Li, M. Gao, R. Hu, Z. Zhao, A. Qin, J. Ling and B. Z. Tang, *J. Am. Chem. Soc.*, 2017, **139**, 5437–5443.
- E. Babu, P. Muthu Mareeswaran, V. Sathish, S. Singaravadevel and S. Rajagopal, *Talanta*, 2015, **134**, 348–353.
- G. Lv, A. Sun, M. Wang, P. Wei, R. Li and T. Yi, *Chem. Commun.*, 2020, **56**, 1625–1628.
- Z. Du, D. Yu, X. Du, P. Scott, J. Ren and X. Qu, *Chem. Sci.*, 2019, **10**, 10343–10350.
- F. L. Heppner, R. M. Ransohoff and B. Becher, *Nat. Rev. Neurosci.*, 2015, **16**, 358–372.
- X.-D. Pan, Y.-G. Zhu, N. Lin, J. Zhang, Q.-Y. Ye, H.-P. Huang and X.-C. Chen, *Mol. Neurodegener.*, 2011, **6**, 45.
- J. Koenigsknecht-Talboo and G. E. Landreth, *J. Neurosci.*, 2005, **25**, 8240–8249.
- M. Kuragano, R. Yamashita, Y. Chikai, R. Kitamura and K. Tokuraku, *Sci. Rep.*, 2020, **10**, 9742.